Published in final edited form as:
Anal Chim Acta. 2006 July 14; 572(1): 1–10. doi:10.1016/j.aca.2006.05.009.

Novel potentiometric and optical silver ion-selective sensors with subnanomolar detection limits

Zsófia Szigeti[a], **Adam Malon**[a], **Tamás Vigassy**[a], **Viktor Csokai**[b], **Alajos Grün**[b], **Katarzyna Wygladacz**[c], **Nan Ye**[c], **Chao Xu**[c], **Vincent J. Chebny**[d], **István Bitter**[b,*], **Rajendra Rathore**[d,*], **Eric Bakker**[c,*], and **Ernö Pretsch**[a,*]

[a] Laboratorium für Organische Chemie, ETH Hönggerberg, CH-8093 Zürich, Switzerland [b] Department of Organic Chemical Technology, Budapest University of Technology and Economics, H-1521 Budapest, Hungary [c] Department of Chemistry, Purdue University, West Lafayette, IN 47907, USA [d] Department of Chemistry, Marquette University, PO Box 1881, Milwaukee, WI 53210-1881, USA

Abstract

Ten Ag^+-selective ionophores have been characterized in terms of their potentiometric selectivities and complex formation constants in solvent polymeric membranes. The compounds with π-coordination show much weaker interactions than those with thioether or thiocarbamate groups as the coordinating sites. Long-term studies with the best ionophores show that the lower detection limit of the best Ag^+ sensors can be maintained in the subnanomolar range for at least one month. The best ionophores have also been characterized in fluorescent microspheres. The so far best lower detection limits of 3×10^{-11}M (potentiometrically) and 2×10^{-11}M Ag^+ (optically) are found with bridged thiacalixarenes.

Keywords

Ion-selective electrodes; Fluorescent microspheres; Silver sensors; Complex formation constants; Lower detection limit; Long-term stability

1. Introduction

Since the description of the first Ag^+-selective ionophore in 1986 [1], at least 50 different lipophilic ligands have been applied in Ag^+-selective membranes (earlier contributions are covered in [2,3]; for a selection of more recent papers, see [4–16]{Johnson, 2002 #21}{Kim, 2005 #56}{Zhang, 2006 #55}). In spite of this large number of compounds, there is an ongoing interest in developing highly selective lipophilic complexing agents for Ag^+ [13–15,17–19]. In most of the approaches, sulfur was used as the coordinating site, mainly in a thioether or thiocarbonyl group. Nitrogen as coordinating site has been used only in a few cases such as in pyridophanes [20] or tetraazacrown ethers [21]. Another group of chelators, applied more recently in polymeric membrane electrodes [9,22–24], is based on π-electrons as the coordinating sites for Ag^+ (see, e.g., [25,26]). Such ionophores seem especially attractive for Ag^+-sensors, since π-electrons do not significantly interact with most of the other ions.

*Corresponding authors: ibitter@mail.bme.hu (I. Bitter), rajendra.rathore@marquette.edu (R. Rathore), bakkere@purdue.edu (E. Bakker), pretsche@ethz.ch (E. Pretsch).

When comparing the selectivity behavior of different ion-selective electrodes (ISEs), it is important that the data is not biased by leaching of primary ions from the membrane into the sample. Unbiased selectivity coefficients can be obtained either by measuring the calibration curves for discriminated ions before the first contact of the membrane with the primary ion [27] or by using appropriate inner solutions [28]. The response slopes for the interfering ions must be recorded since close to theoretical values confirm that selectivity coefficients are not biased [29]. Unfortunately, Ag^+-ISEs have only recently been characterized under such precautions [8,15,16,30,31] so that the selectivity behavior of most Ag^+-ISEs published earlier is not directly comparable. Similarly, without suppressing ion fluxes in the ISE membranes, the lower detection limit of the sensors is also biased [32,33]. So far, only two papers have reported on Ag^+-ISEs with optimized lower detection limits showing values of 10^{-9} (100 ppt) [30] and 3×10^{-10}M Ag^+ [31].

Besides the standard free energy of transfer, which leads to rather favorable selectivities for Ag^+ in ionophore-free ion-exchanger membranes [34,35], the formal complex formation constants in the membrane phase are the parameters that define the selectivity behavior. They are directly accessible by optical [36] or potentiometric measurements [37] on two membranes, one containing the usual components, i.e., the ionophore, the H^+-selective chromoionophore (which is assumed not to bind ions other than H^+), and the lipophilic anionic sites, and the other without ionophore but otherwise of the same composition. Another possibility is to measure the selectivity coefficient of the target ion relative to a reference ion that does not interact with the ionophore (e.g., a tetraalkylammonium ion), using the conventional ionophore-based membrane together with a second membrane that contains only the ion exchanger but no ionophore [38]. Finally, the complex formation constant is directly accessible also from the transmembrane potential of a symmetrically bathed double membrane obtained by joining two preconditioned membranes, one of the usual composition and the other again containing the ion exchanger without the ionophore (sandwich membrane method [39,40]). So far, complex formation constants of only a few Ag^+-selective ionophores have been determined by such methods [15,31,39].

In this contribution, we investigate the potentiometric behavior of six recently synthesized Ag^+ ionophores, which have not yet been characterized in ISE membranes, and compare it with that of four further ones, which have earlier been applied in ISEs. The complex formation constants with Ag^+ are determined in the membrane phase. Based on the selectivity behavior, lower detection limit, and stability of the responses, the most promising ISEs are selected and also characterized as optical sensors in fluorescent microspheres. From these studies, the ionophore with the best performance in terms of selectivity behavior and long-term stability is selected with a view of trace measurements in confined samples {Malon, 2006 #54}.

2. Experimental

2.1. Reagents

Poly(vinyl chloride) (PVC), bis(2-ethylhexyl) sebacate (DOS), 2-nitrophenyl octyl ether (*o*-NPOE), sodium tetrakis[3,5-bis(trifluoromethyl)phenyl]borate (NaTFPB), 9-(dimethylamino)-5-[4-(15-butyl-1,13-dioxo-2,14-dioxanonadecyl)-phenyl-imino]benzo[a] phenoxazine (ETH 5418, chromoionophore VII), tetrahydrofuran (THF, puriss. p.a.) were Selectophore®, tetraethylammonium nitrate (Et_4NNO_3) and the other salts were puriss. p.a., all from Fluka (CH-9471 Buchs, Switzerland or Milwaukee, WI, USA), HNO_3 solution was Titrisol® from Merck (Darmstadt, Germany), methylene chloride, ethyl acetate, and xylene from Fisher Chemical (Fair Lawn, NJ, USA), cyclohexanone (99.8%) and tris(hydroxymethyl) aminomethane (Tris) from Sigma-Aldrich (St. Louis, MO, USA); 3-morpholinopropanesulfonic acid (MOPS) and magnesium acetate were from Fluka (Milwaukee, WI, USA). The internal reference dye, 1,1′-dioctadecyl-3,3,3′,3′-

tetramethylindocarbocyanine perchlorate (DiIC18) was from Molecular Probes (Eugene, OR, USA). Ionophore **VI** ([2.2.2]paracyclophane; for structures, see Figures 1, 2) was from Merck, **VII** (5,11,17,23-tetra-*tert*-butyl-25,27-di(2-methylthio)ethoxycalix[4]arene) [41] and **VIII** (o-xylene-bis-(*N*,*N*-diisobutyldithiocarbamate) were from Fluka (Selectophore®), respectively. The other ionophores were synthesized according to published procedures: **I** (5,11,17,23-tetra-*tert*-butyl-25,26,27,28-tetraallyloxycalix[4]arene [42]), **II** (5,11,17,23-tetra-*tert*-butyl-25,27-diallyloxy-26,28-dibenzyloxycalix[4]arene [42]), **III** (5,11,17,23-tetra-*tert*-butyl-25,27-diallyloxy-26,28-dipropoxycalix[4]arene [42]), **IV** (1,3-*alt*-25,26,27,28-tetraallyloxy-4-*tert*-butylthiacalix[4]arene [43]), **V** (1,4-bis[(9-methyl-9*H*-fluoren-9-yl)methyl]benzene [17]), **IX** (1,3-*alt*-5,11,17,23-tetra-*tert*-butyl-25,27-dipropoxy-26,28-(3,9-dithia-6-oxaundec-1,11-diyloxy)thiacalix[4]arene [44]), and **X** (1,3-*alt*-5,11,17,23-tetra-*tert*-butyl-25,27-di-*n*-octyloxy-26,28-[pyridine-2,6-bis(methylthioethoxy)]thiacalix[4]arene [44]). Aqueous solutions were prepared with freshly deionized water (specific resistance, >18 M Ω cm, pH 5.5) from a NANOpure® reagent grade water system (Barnstead, CH-4009 Basel, Switzerland).

2.2. ISE membranes and electrodes

The membrane compositions are listed in Table 1. The membrane components (totaling ca. 260 mg) were dissolved in THF (2.0 mL) during ca. 2 h and poured into a glass ring (37 mm i.d.) fixed on a glass plate and covered with another glass plate. After overnight evaporation of the solvent at RT, disks of 5 mm in diameter were punched from the master membrane (thickness, ca. 200 μm) and glued with a PVC/THF slurry to a plasticized PVC tubing mechanically fixed onto a 1000-μL pipette tip. The inner filling solution for selectivity measurements was 10^{-2}M $NaNO_3$ and for optimal lower detection limits and long term experiments it was 10^{-3}M Et_4NNO_3 with $10^{-5.5}$ or $10^{-6.4}$M $AgNO_3$ with the *o*-NPOE/PVC or DOS/PVC membranes, respectively. The Ag/AgCl inner reference electrode in 10^{-2}M NaCl was separated from the internal solutions by a diaphragm. The sandwich membrane experiments were performed with Philips electrode bodies as described in [39] using 10^{-3}M $AgNO_3$ as internal solution.

2.3. EMF measurements

Measurements were performed with a 16-channel electrode monitor (Lawson Labs Inc., Malvern, Pa 19355, USA) in magnetically stirred solutions at RT. Activity coefficients were calculated according to the Debye–Hückel approximation and EMF values were corrected for liquid-junction potentials with the Henderson equation. Sample pH values were determined with a Metrohm glass electrode (No. 6.0133.100, Metrohm AG, CH-9010 Herisau, Switzerland). All dilute solutions ($<10^{-4}$ M) were freshly prepared. Each concentration and salt had its own polyethylene container assigned. The reference electrode was a Metrohm double junction Ag/AgCl type No. 6.0729.100 with 3 M KCl as reference and 1 M NH_4NO_3 as bridge electrolyte.

2.4. Selectivity measurements

Selectivity coefficients were measured with 3 ISEs of each membrane after conditioning them for 1 d in 10^{-2}M $NaNO_3$. The sequence of the sample ions was Na^+, Ca^{2+}, H^+, Ag^+, and Et_4N^+, or K^+, Li^+, Mg^{2+}, Pb^{2+}, Cu^{2+}, Hg^{2+}, and Ag^+. First, measurements were made in the respective 10^{-2} or 10^{-3}M nitrate solutions and, after reaching sufficiently stable potentials (drift <0.5 mV/10 min), 2 more points were taken at lower concentrations. When required (e.g., for Hg^{2+} and Pb^{2+}), the pH of the solutions was adjusted with HNO_3 to avoid precipitation of insoluble species such as hydroxide or carbonate. The selectivity coefficients were calculated from the EMF values obtained in the most concentrated nitrate solutions according to the separate solution method assuming theoretical slopes [29,45].

2.5. Potentiometric determination of complex formation constants

The complex formation constants (β_{IL_n}) were determined either from selectivity measurements using Et_4N^+ as reference ion according to equation 3 in [38] with an assumed value of n = 1 as the stoichiometric factor and a measured selectivity coefficient of log K^{pot}_{Ag,Et_4N}=5.06 ± 0.01 for the ionophore-free membrane. Alternatively, the segmented sandwich technique was used according to reference [39]. The conditioning, measuring, and internal solutions were 10^{-3} M $AgNO_3$. Because of using a polar plasticizer (*o*-NPOE), no formation of ion pairs in the membrane was considered (β_{IL_n} was calculated according to equation 10 in [39]).

2.6. ISEs for optimal lower detection limit and long-term measurements

Optimal lower detection limits and long-term measurements were studied with 3 ISEs of the membrane with ionophore **IX** (cf. Table 1) after conditioning them for 2 d in 10^{-5}M $AgNO_3$ and then for 1 d in 10^{-8}M $AgNO_3$ without background. For long-term measurements, the ISEs were kept in the dark in 10^{-8}M $AgNO_3$. Calibration curves were taken by successively diluting solutions from 10^{-5} to 10^{-11} or 10^{-12}M $AgNO_3$, readings being taken after sufficiently stable EMF values had been reached (drift <0.5 mV/10 min).

2.7. Preparation of fluorescent microspheres

Fluorescent microspheres were prepared using a previously described sonic particle-casting apparatus [31]. The casting procedure is based on the coexistence of two streams, a diluted membrane cocktail (core) and purified water (sheath). The membrane cocktail containing the sensing ingredients, i.e., 30 mmol/kg of **IX** or **X** with 2 mmol/kg of ETH 5418, 0.025 mmol/kg of DiIC18, and 3.4 mmol/kg of NaTFPB, was dissolved in cyclohexanone (2.5 mL), diluted with methylene chloride (50 mL), and filtered with a 0.45-μm syringe filter to remove any solid impurities. Both streams were directed to the mixing chamber of the particle caster. The organic core stream was broken into droplets by oscillating a piezoelectric crystal and polymeric particles were formed after curing. The following setup was applied: a ceramic tip with a 0.0017″ diameter orifice, a 0.7 mL/min water stream flow rate, 16 kHz oscillator frequency, and a 0.5 mL/min polymer flow rate. Microspheres suspended in the receiving water phase were collected in 10-mL glass vials. After casting, the microspheres were stored in the dark for several hours to allow the microspheres to settle at the bottom of the glass vials.

2.8. Optical measurements

A PARISS Imaging Spectrometer (Light Form, Belle Mead, NJ, USA) in combination with a Nikon Eclipse E400 microscope was used to characterize the microspheres as described previously [31].

Calibration curves and selectivities were recorded in 1 mM buffer solutions (Tris-HNO_3 or MOPS-NaOH at pH 7.4 and magnesium acetate buffer at pH 4.7) containing the appropriate electrolytes. All calibrating solutions were placed in polyethylene beakers that had been pretreated with 0.01 M HNO_3. The calibration curve for Ag^+ was recorded in a 0.8 mM sodium nitrate background.

Microspheres immobilized on glass slides were normally equilibrated in 100 mL of buffered sample solutions for at least 1 h before measurement. Calibration curves were recorded in 10^{-11}–10^{-8}M (**X**) or 10^{-9}–10^{-6}M (**IX**) $AgNO_3$ solutions buffered at pH 4.7 and 7.4. Selectivity coefficients were evaluated using the separate solutions method (SSM) from the horizontal distance between logarithmic activities of primary and interfering ions at α = 0.5 and pH 7.4.

The exposure time for the fluorescence data acquisition was 200 ms. To minimize photobleaching, a neutral density filter ND 4 was used. The spectra of the fully protonated and

fully unprotonated chromoionophore, ETH 5418, were recorded at 10 mM HCl and 10 mM NaOH, respectively. Ratiometric measurements were performed by comparing the fluorescence emission peaks of ETH 5418 and the reference dye, DiIC18, at 709 and 612 nm, respectively. For experimental details and spectra, see ref. {Wygladacz, 2005 #39}.

3. Results and Discussion

The characteristics of sensing membranes based on ten Ag^+-selective ionophores are investigated here in order to choose the best ones in terms of selectivity, lower detection limit, and stability of the responses. Six of them, four with π-electrons as coordinating sites (**II**–**V**) and two with thioethers (**IX**, **X**), had not been characterized previously in sensing membranes. For comparison, two further π-coordinating ligands (**I**, **VI**) and the two ionophores that, so far, had given the best lower detection limits (**VII**, **VIII**) were selected. Since first tests revealed significantly better Ag^+ selectivities in *o*-NPOE- than in DOS-based membranes, the former plasticizer was chosen for screening experiments. In a first step, selectivity coefficients were determined for H^+, Na^+, Ca^{2+}, and Et_4N^+ (see Tables 2, 3 and Figures 1, 2). Then, with ionophores **VII**–**X**, which led to a much better selectivity behavior than all the others, the selectivity coefficients were determined also for further relevant ions (Table 3).

The selectivity coefficients of membranes containing a π-coordinating ionophore (**I**–**VI**) are significantly less good for all investigated ions than those of **VII**–**X** (see Tables 2, 3). In contrast to ISEs with ionophores **VII**–**X**, those with **I**–**VI** are selective for Et_4N^+. Ionophore **IV** has the poorest performance. This might be because, in contrast to the other calix[4]arene derivatives, it does not have a cone conformation [43]. ^1H NMR measurements performed in $CDCl_3$ with ligand **IV** in the presence of Ag^+ revealed that the two allyl groups in 1,3-*alt* conformation are not sufficient for binding, probably because the adjacent phenyl rings are not arranged in parallel position due to steric hindrance of the bulky *tert*-butyl groups, so that they cannot stabilize Ag^+ by additional π-cation interaction. At the same time, upon complexation, a conformational change to *paco* (partial cone) has been observed affording three allyl groups in *syn* position capable of efficient Ag^+ binding as reflected by the significant downfield shifts of the CH_2=CH protons [43]. We assume that this process readily taking place with **IV** in solution is kinetically inhibited in the membrane phase, thus degrading its selectivity performance. It could be also explained by the fact that the corresponding membrane was turbid indicating that some components were not fully dissolved. The high preference of Et_4N^+ may indicate that partial crystallization of **IV** caused an excess of ion exchanger in the membrane [46]. The rather poor Ag^+ selectivity of **V** relative to that of **VI** is surprising (see below).

In Fig. 2 and Table 3, the, so far, best Ag^+ ionophores, **VII** and **VIII**, are compared with two recently synthesized bridged thiacalix[4]arenes, **IX** and **X**. Except for the reduced H^+ selectivity of **X** (log $K^{pot}_{AgH} = -6.7$ as compared to <−10 for **VIII** and **IX** in *o*-NPOE/PVC membranes), the performance of these four ionophores is similar. Note that with **X**, no responses are obtained for Na^+, Mg^{2+}, and Ca^{2+} since H^+ is the potential-determining ion during these measurements. Therefore, only limiting values can be given for the corresponding selectivity coefficients (Table 3). Apart from **VIII**, Hg^{2+} is also rather strongly discriminated. With ISEs containing **VIII**, no calibration curve could be obtained for Hg^{2+}, which caused strongly drifting potentials that did not significantly depend on its concentration. Most probably, the thiocarbonyl groups of **VIII** react with Hg^{2+}. Earlier, we had similar problems with another ligand having such groups in the presence of Cu^{2+} [47].

In most cases, super-Nernstian responses have been observed for Et_4N^+ (see Tables 2 and 3). This can be explained by the applied measurement protocol according to which, first, the responses for discriminated ions are recorded and only after that for the primary ion {Bakker, 1997 #36}. It has been shown that about 30 min after the first contact with the primary ion, a

long-term negative potential drift occurs, which can be explained by a change in the inner phase-boundary potential. Since in the present study, the response to Et_4N^+ was always recorded after that to Ag^+, the slow downward drift leads to a super-Nernstian response function. This effect should not have any significant influence on the selectivity coefficient since it was always calculated from the EMF value of the most concentrated solution (which was always measured first) and theoretical slopes were used in the calculations.

Formal complex formation constants, log β, of Ag^+ have been determined for all ionophores (Table 4), based on the respective selectivity coefficients for Et_4N^+ (Table 3) and using log $K^{pot}_{AgEt_4N} = 5.06 \pm 0.01$ (S.D., $n = 3$) determined for the *o*-NPOE/PVC membrane without any ionophore. Additionally, for ionophores **I** and **VII**–**X**, the segmented sandwich membrane technique was used for determining log β (Table 4). Except for **I**, the deviations between the values obtained with the two methods are statistically not significant at the 99.5% confidence level. The satisfactory agreement of the values obtained with the two methods indicates that Et_4N^+ does not significantly interact with the ionophores. One possible exception is **I**, for which the selectivity method led to an about 10 times weaker interaction with Ag^+. It is apparent that all ionophores with π-electrons as coordinating sites (**I**–**VI**) have complex formation constants that are lower by 4–6 orders of magnitude than those with S as the coordinating site. This explains their inferior overall selectivity behavior. It is surprising that the formal complex formation constant of **V** with Ag^+ is about 300 times lower than that of **VI** since in a competition experiment with a 1:1 mixture of both ionophores and 0.5 equivalents of Ag^+, the ^{1}H NMR spectrum indicated that **V** was complexed and **VI** was not [17]. However, in that experiment in the rather apolar solvent $CDCl_3$, the counterion was $CF_3SO_3^-$, whereas the sensor membrane investigated here is based on the polar *o*-NPOE (dielectric constant, 23.9 [48]) and the counterion is a substituted tetraphenylborate, $TFPB^-$. A likely explanation of the observed difference is that the ion pairs with $CF_3SO_3^-$ in $CDCl_3$ are strong, whereas with $TFPB^-$ in *o*-NPOE they are weak [39]. Since the steric shielding by **VI** is probably much stronger than by **V**, formation of the strong ion pairs stabilizes the complex of **V** to a much larger extent. Another possible explanation would be that **V** forms some invisible aggregates in the membrane [46]. For membranes with ionophores **VII**–**X**, the values of log β are similar (for *o*-NPOE/PVC membranes $>10^{10}$). They are of the same order as those found with the best ionophores for monovalent ions [49] and also similar to that determined recently with a tripodal *N*-acylthiourea ionophore ($10^{11.7}$) [15].

Long-term measurements with the ionophores **VII**–**IX** showed that **IX** has the best performance. With this ligand, the response curve changed only slightly after 62 d relative to day 7, and the EMF difference between 10^{-5} and 10^{-11}M Ag^+ remained constant. This EMF difference changed by about 30 mV between day 6 and 48 for membranes with **VII** and by 100 mV for those with **VIII** (results not shown). Due to its good stability, further measurements were made with **IX** and both with *o*-NPOE and DOS as the plasticizer (Fig. 3). The two internal solutions (see Experimental, section 2.2) induced an exchange of 9% of Ag^+ by Et_4N^+ on the inner membrane side. Owing to the higher than usual PVC content (see Table 1), they did not induce any super-Nernstian response. The lower detection limit was 3×10^{-11} and 5×10^{-10}M Ag^+ (i.e., log $a_{Ag+} = -10.6$ and -9.3, see Fig. 3) with the *o*-NPOE/PVC and DOS/PVC membranes, respectively. The value obtained with *o*-NPOE is better by about one order of magnitude than the best one obtained so far [30,31]).

Optode microspheres of DOS-plasticized PVC were characterized with the appropriate salts in solutions buffered with MOPS (pH 7.4) or magnesium acetate (pH 4.7). The response times were similar to those recently obtained with such microspheres {Wygladacz, 2005 #39}. For example, the response time in a 10^{-9}M Ag^+ solution was 30 min. Theoretical curves (solid lines) were computed using the same values of log K^{Ag}_{exch} [50] (−1.0 for **IX** and +0.9 for **X**,Fig.

4). The corresponding stability constants estimated from these exchange constants and from that obtained for the optode without ionophore, i.e., log $K^{Ag}_{exch} = -8.8$, were found as log β = 9.7 (**IX**) and log β = 7.8 (**X**). These values are lower by about 2–3 orders of magnitude than for PVC membranes plasticized with *o*-NPOE (Table 4). Similarly, the value determined earlier with the segmented sandwich membrane technique for DOS/PVC membranes with **VIII** (log β = 9.22) is lower by about two orders of magnitude than for the analogous *o*-NPOE/PVC membranes used here. These results are in line with previous observations on a series of other ionophores [49].

The responses of optode microspheres with **IX** or **X** at pH 7.4 to a series of interfering ions are shown in Fig. 5, the corresponding selectivity coefficients and exchange constants in Table 5 {Bakker, 1997 #50}. Although the potentiometric and optical selectivity coefficients are, in general, fundamentally different {Bakker, 1997 #50}, the selectivity coefficients of these DOS-based optodes show a reasonable correlation with those obtained potentiometrically (Table 3). Note, however, that the optical measurements with **X** give unbiased selectivity coefficients also for Na^+, Mg^{2+}, and Ca^{2+} since with the optodes used here, there is no interference by H^+.

The reversibility of optical responses of **IX** and **X** was studied with optode films having analogous compositions to those of the fluorescent microspheres. First, the chromoionophore (ETH 5418) was fully protonated by equilibrating the membrane with 0.01 M HCl. An immediate color change from pink to green took place. Then, the films were gently dried and a few droplets of 10^{-4}M $Hg(NO_3)_2$ were pipetted onto them, upon which their color changed from green to pink due to the deprotonation of the dye. However, this color change due to the complexation of Hg^{2+} by the ionophore was much slower in the case of the films containing **X** (ca. 5 min) than with **IX** (ca. 2 min). To check the reversibility, the films were rinsed with deionized water and reexposed to 0.01 M HCl. For both ionophores, the process is fully reversible but again, a longer time was required to reach the equilibrium with films based on **X** (ca. 30 min) than with **IX** (ca. 3 min).

Interestingly, the lower detection limit of 5×10^{-9}M Ag^+ for the DOS/PVC optode microspheres based on **IX** was inferior by about one order of magnitude than that observed potentiometrically with the corresponding ISE membranes (see above). On the other hand, the lower detection limit of 2×10^{-11}M Ag^+ for the analogous optode microspheres based on **X** was better than that obtained with the corresponding ISE.

4. Conclusions

In this contribution, unbiased selectivity coefficients have been determined for ten Ag^+-selective ionophores. Although ligands with π-coordination show only negligible interactions with most interfering cations compared with those having S as coordinating sites, their selectivity behavior is inferior. This unexpected performance is shown to be the consequence of much weaker complexes formed with π-coordinating ligands than with S-coordinating ones. Concerning their selectivity behavior, lower detection limit, and response stability, the best performance was achieved with a recently synthesized bridged thiacalix[4]arene derivative. The potentiometric lower detection limit of 3×10^{-11}M Ag^+ for an *o*-NPOE/PVC membrane is the best reported so far. With optode microspheres based on DOS/PVC, another related bridged thiacalix[4]arene derivative had the best performance, exhibiting a lower detection limit of 2×10^{-11}M Ag^+.

Acknowledgments

This work was financially supported by the Swiss National Science Foundation, an internal research grant of the ETH Zurich, the National Institutes of Health (grants EB002189 and DE14950), and the National Science Foundation (Career Award). Financial support by the Hungarian Scientific Research Found (OTKA No. T 046055) is gratefully acknowledged. V. Csokai thanks the Zoltán Magyary fellowship. We thank Dr. D. Wegmann for careful reading of the manuscript.

References

1. Lai MT, Shih JS. Analyst 1986;111:891.
2. Bühlmann P, Pretsch E, Bakker E. Chem Rev 1998;98:1593. [PubMed: 11848943]
3. Bakker E, Bühlmann P, Pretsch E. Electroanalysis 1999;11:915.
4. Bryce MR, Johnston B, Kataky R, Tóth K. Analyst 2000;125:861.
5. Xu D, Katsu T. Anal Chim Acta 2001;443:235.
6. Chen L, He X, Zhang H, Liu Y, Hu X, Sheng Y. Anal Lett 2001;34:2237.
7. Yoon I, Lee YH, Lee SS, Lee SC, Park SB. Analyst 2001;126:1773.
8. Johnson RD, Pinchart A, Badr IHA, Gingras M, Bachas LG. Electroanalysis 2002;14:1419.
9. Bobacka J, Lahtinen T, Koskinen H, Rissanen K, Lewenstam A, Ivaska A. Electroanalysis 2002;14:1353.
10. Zeng X, Weng L, Chen L, Xu F, Li Q, Leng X, He X, Zhang ZZ. Tetrahadron 2002;58:2647.
11. Shamsipur M, Javanbakht M, Ganjali MR, Mousavi MF, Lippolis V, Garau A. Electroanalysis 2002;14:1691.
12. Zeng X, Sun H, Chen L, Leng X, Xu F, Li Q, He X, Zhang W, Zhang ZZ. Org Biomol Chem 2003;1:1073. [PubMed: 12929650]
13. Park KM, Lee YH, Jin Y, Seo J, Yoon I, Lee SC, Park SB, Gong MS, Seo ML, Lee SS. Supramol Chem 2004;16:51.
14. Shim JH, Jeong IS, Lee MH, Hong HP, Ona JH, Kim KS, Kim HS, Kim BH, Cha GS, Nam H. Talanta 2004;63:61. [PubMed: 18969404]
15. Reinoso-García MM, Dijkman A, Verboom W, Reinhoudt DN, Malinowska E, Wojciechowska D, Pietrzak M, Selucky P. Eur J Org Chem 2005:2131.
16. Badr IHA. Mikrochim Acta 2005;149:87.
17. Rathore R, Chebny VJ, Abdelwahed SH. J Am Chem Soc 2005;127:8012. [PubMed: 15926815]
18. Jiménez-Morales A, Galván JC, Aranda P. Electrochim Acta 2002;47:2281.
19. Lu JQ, Pang DW, Zeng XS, He XW. J Electroanal Chem 2004;568:37.
20. Hasse W, Ahlers B, Reinbold J, Cammann K, Brodesser G, Vögtle F. Sens Actuators B 1994;18–19:380.
21. Teixidor F, Flores MA, Escriche L, Vinas C, Casabo J. J Chem Soc Chem Commun 1994:963.
22. Gross J, Harder G, Siepen A, Harren J, Vögtle F, Stephan H, Gloe K, Ahlers B, Cammann K, Rissanen K. Chem Eur J 1996;2:1585.
23. Kimura K, Yajima S, Tatsumi K, Yokoyama M, Oue M. Anal Chem 2000;72:5290. [PubMed: 11080878]
24. Bobacka J, Lahtinen T, Nordman J, Haggstrom S, Rissanen K, Lewenstam A, Ivaska A. Electroanalysis 2001;13:723.
25. Pierre JL, Baret P, Chautemps P, Armand M. J Am Chem Soc 1981;103:2986.
26. Kang HC, Hanson AW, Eaton B, Boekelheide V. J Am Chem Soc 1985;107:1979.
27. Bakker E. Anal Chem 1997;69:1061.
28. Sokalski T, Ceresa A, Fibbioli M, Zwickl T, Bakker E, Pretsch E. Anal Chem 1999;71:1210.
29. Bakker E, Pretsch E, Bühlmann P. Anal Chem 2000;72:1127. [PubMed: 10740849]
30. Ceresa A, Radu A, Peper S, Bakker E, Pretsch E. Anal Chem 2002;74:4027. [PubMed: 12199570]
31. Wygladacz K, Radu A, Xu C, Qin Y, Bakker E. Anal Chem 2005;77:4706. [PubMed: 16053279]
32. Mathison S, Bakker E. Anal Chem 1998;70:303.

33. Sokalski T, Ceresa A, Zwickl T, Pretsch E. J Am Chem Soc 1997;119:11347.
34. Brzózka Z, Cobben PLHM, Reinhoudt DN, Edema JJH, Buter N, Kellogg RM. Anal Chim Acta 1993;273:139.
35. Wróblewski W, Brzózka Z. Sens Actuators B 1995;24–25:183.
36. Bakker E, Willer M, Lerchi M, Seiler K, Pretsch E. Anal Chem 1994;66:516.
37. Bakker E, Pretsch E. Anal Chem 1998;70:295.
38. Ceresa A, Pretsch E. Anal Chim Acta 1999;395:41.
39. Mi Y, Bakker E. Anal Chem 1999;71:5279. [PubMed: 10596210]
40. Shultz MM, Stefanova OK, Mokrov SB, Mikhelson KN. Anal Chem 2002;74:510. [PubMed: 11838668]
41. Cobben PLHM, Egberink RJM, Bomer JB, Bergveld P, Verboom W, Reinhoudt DN. J Am Chem Soc 1992;114:10573.
42. Bitter I, Grün A, Agai B, Töke L. Tetrahedron 1995;51:7835.
43. Csokai, V.; Grün, A.; Simon, A.; Balazs, B.; Tóth, G.; Bitter, I. Tetrahedron. 2006. submitted
44. Csokai V, Bitter I. Supramol Chem 2004;16:611.
45. Guilbault GG, Durst RA, Frant MS, Freiser H, Hansen EH, Light TS, Pungor E, Rechnitz G, Rice NM, Rohm TJ, Simon W, Thomas JDR. Pure Appl Chem 1976;48:127.
46. Phillips KN, Lantz C, Bühlmann P. Electroanalysis 2005;17:2019.
47. Szigeti Z, Bitter I, Tóth K, Latkoczy C, Fliegel DJ, Günther D, Pretsch E. Anal Chim Acta 2005;532:129.
48. Dinten O, Spichiger UE, Chaniotakis N, Gehrig P, Rusterholz B, Morf WE, Simon W. Anal Chem 1991;63:596. [PubMed: 2031561]
49. Qin Y, Bakker E. Anal Chim Acta 2000;421:207.
50. Bakker E, Bühlmann P, Pretsch E. Chem Rev 1997;97:3083. [PubMed: 11851486]

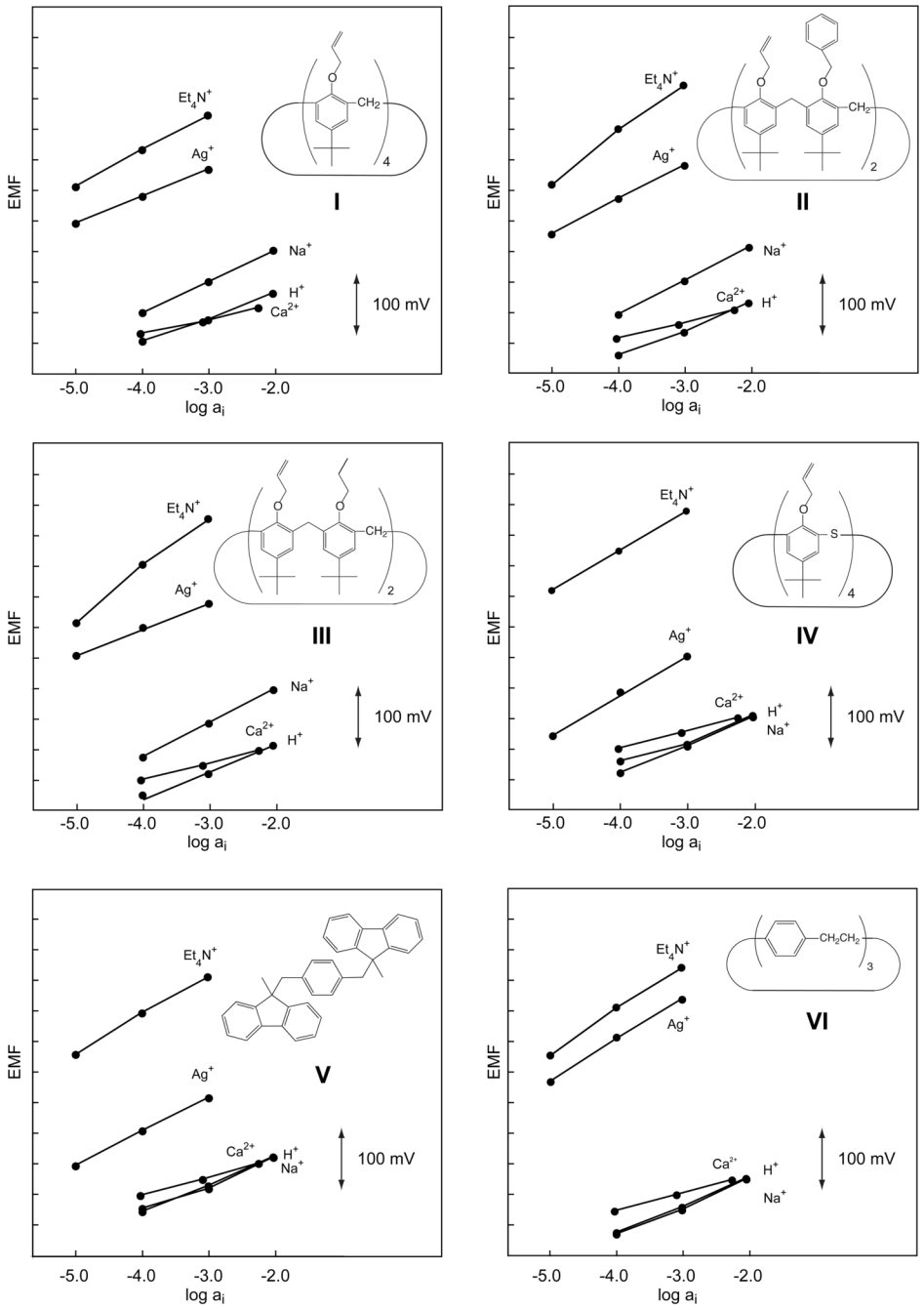

Figure 1.
Potentiometric response behavior of the six Ag^+-selective ionophores, **I**–**VI**, having π-electrons as coordinating sites.

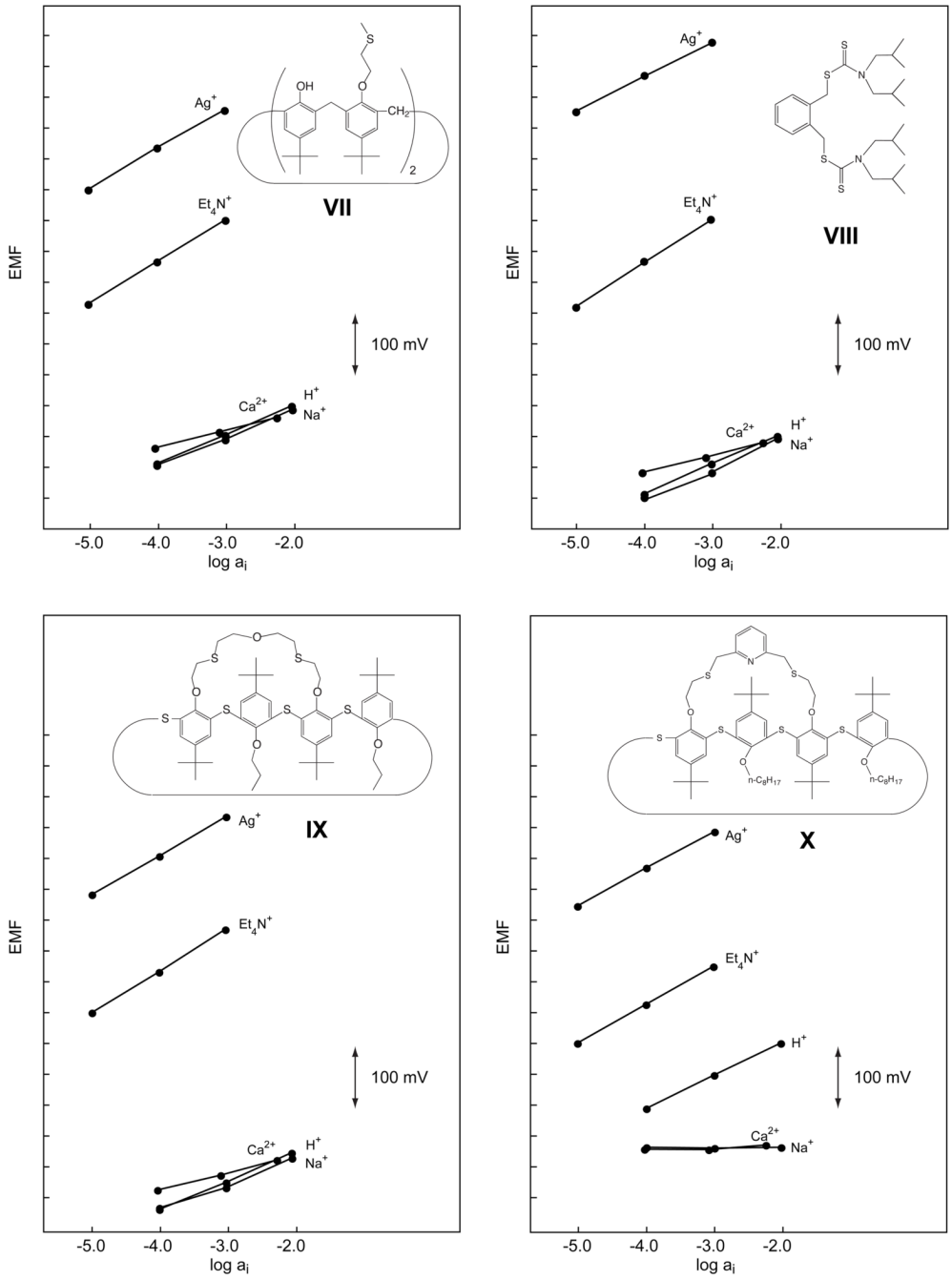

Figure 2.
Potentiometric response behavior of the four Ag^+-selective ionophores, **VII**–**X**, having S as coordinating sites.

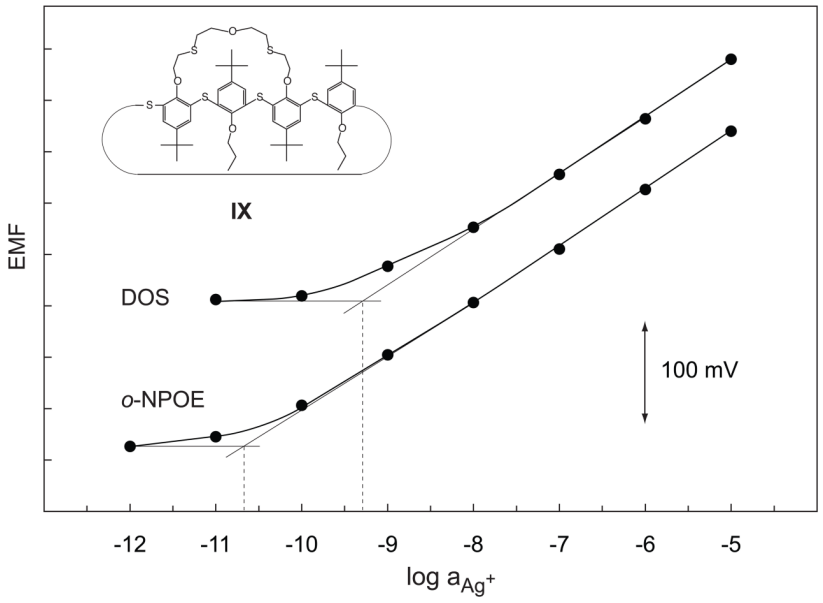

Figure 3.

Calibration curves obtained with *o*-NPOE/PVC and DOS/PVC membranes based on ionophore **IX**. The lower detection limits are 3×10^{-11} and 5×10^{-10}M Ag^+ (i.e., log $a_{Ag+} = -10.6$ and −9.3), respectively.

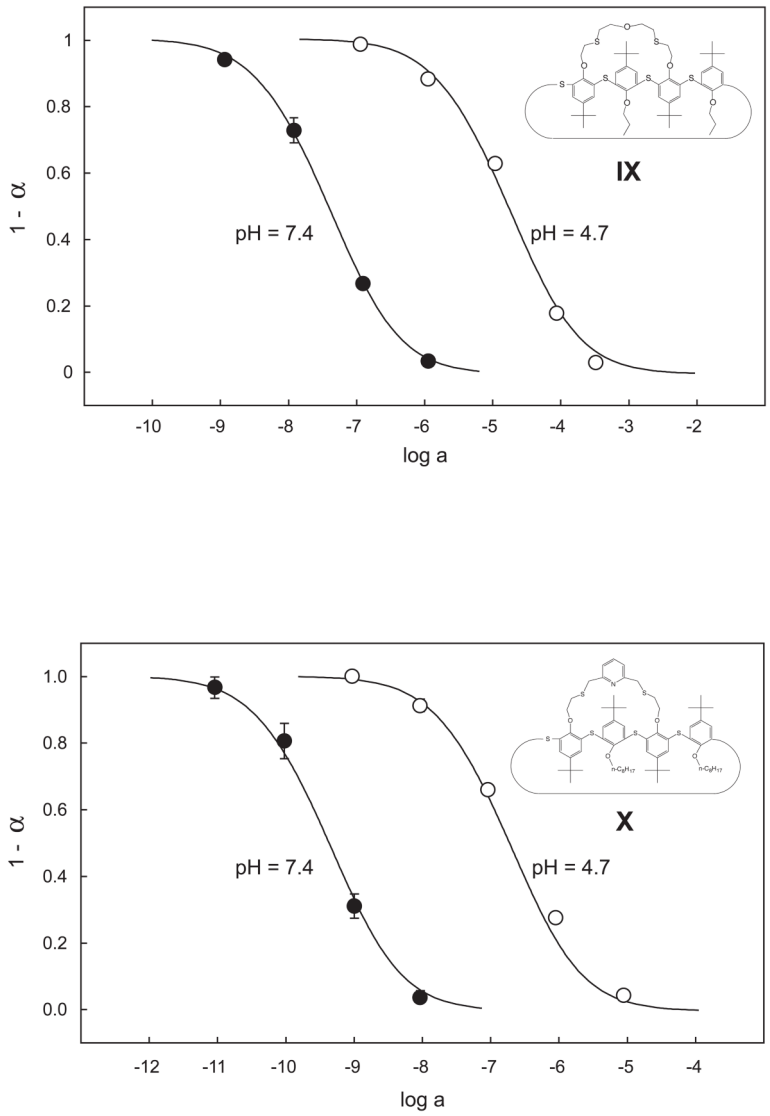

Figure 4.

Optical response of DOS/PVC microspheres based on ionophore **IX** (top) and **X** (bottom) expressed as the mole fraction of the protonated chromoionophore (ETH 5418, see Experimental). The sensing particles were immobilized on glass slides. The $AgNO_3$ solutions were applied in $Mg(OAc)_2$ buffer at pH 4.7 or MOPS buffer at pH 7.4. The theoretical response curves (solid lines) were calculated with the same exchange constant at both pH values.

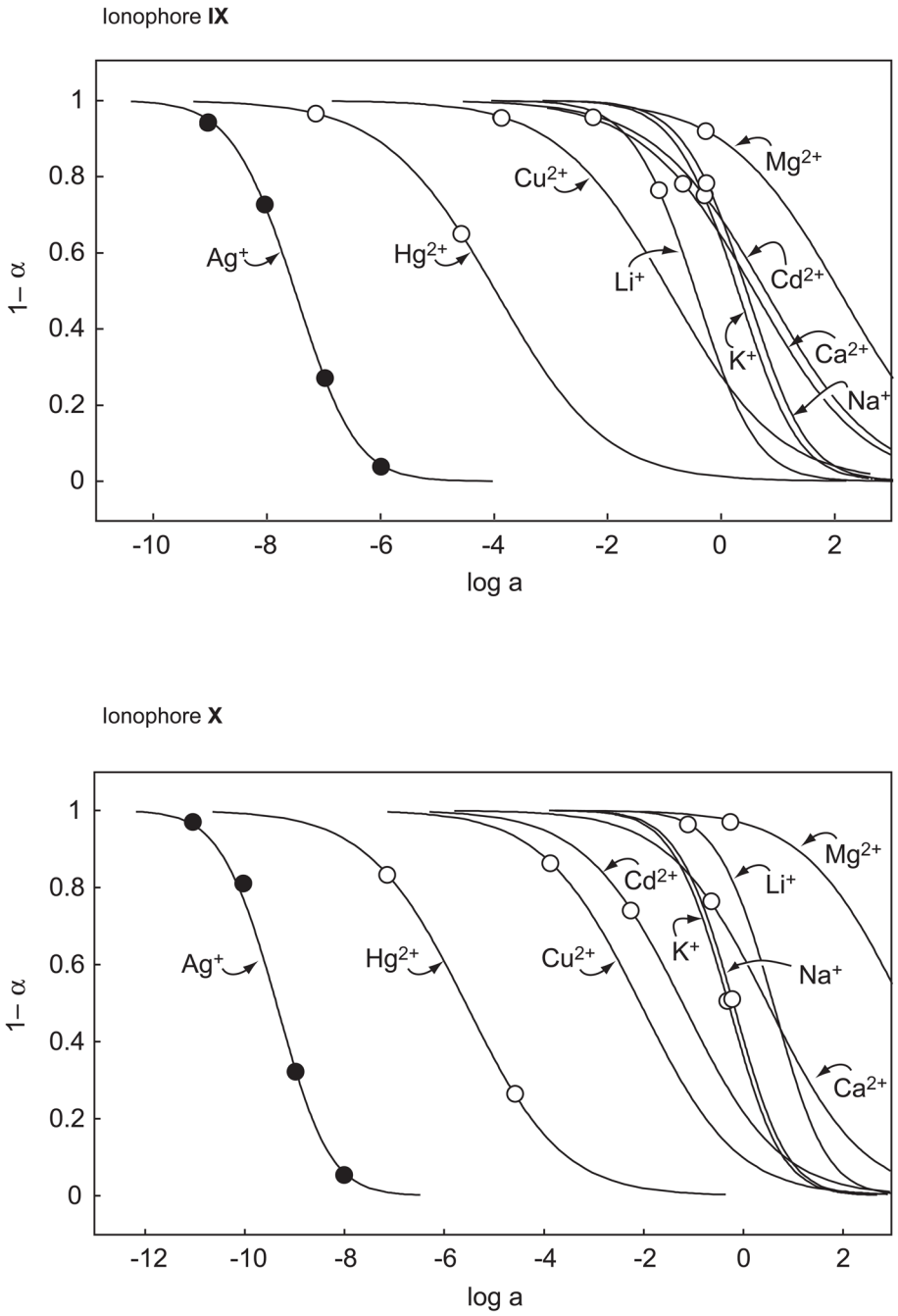

Figure 5.

Optical response behavior of DOS/PVC microspheres based on ionophore **IX** (top) and **X** (bottom) to different ions at pH 7.4. The theoretical curves (solid lines) were calculated with the exchange constants, $K_{\text{exch}}^{\text{Ag}}$, given in Table 5.

Table 1

Composition of the membranes

Ionophore	Ionophore wt% (mmol/kg)	NaTFPB wt% (mmol/kg)	PVC wt%	Plasticizer, wt%
I	0.80 (9.87)	0.43 (4.89)	42.1	*o*-NPOE, 56.6
II	0.91 (10.00)	0.44 (4.93)	42.2	*o*-NPOE, 56.5
III	0.83 (10.27)	0.44 (5.00)	43.1	*o*-NPOE, 55.6
IV	0.89 (10.14)	0.44 (4.97)	43.0	*o*-NPOE, 55.6
V	0.47 (10.13)	0.43 (4.89)	42.8	*o*-NPOE, 56.3
VI	0.33 (10.69)	0.45 (5.05)	43.0	*o*-NPOE, 56.3
VII	0.80 (10.05)	0.44 (5.00)	43.1	*o*-NPOE, 55.6
VIII	0.51 (9.96)	0.45 (5.03)	43.0	*o*-NPOE, 56.0
IX	0.99 (9.99)	0.44 (4.98)	43.0	*o*-NPOE, 55.6
	1.00 (10.02)	0.43 (4.83)	42.9	DOS, 55.7
X	1.19 (10.15)	0.44 (4.93)	42.4	*o*-NPOE, 56.0
	1.14 (9.75)	0.42 (4.76)	41.6	DOS, 56.8
Ion exchanger	—	0.44 (5.01)	43.3	*o*-NPOE, 56.3

Table 2

Potentiometric selectivity coefficients, log K^{pot}_{AgJ}, and response slopes (in parentheses; concentration ranges: 10^{-3}–10^{-5}M for Ag^+ and Et_4N^+, 10^{-2}–10^{-4}M for all other ions) obtained with the separate solution method for PVC membranes based on the ionophores **I–VI** (cf. Fig. 1)

Ion J	I	II	III	IV	V	VI
Ag^+	0 (52.9)	0 (56.4)	0 (45.5)	0 (61.4)	0 (58.6)	0 (68.4)
H^+	−4.41 ± 0.03 (40.9)	− 4.75 ± 0.04 (44.2)	−5.15 ± 0.22 (43.1)	−2.59 ± 0.05 (38.1)	−2.73 ± 0.10 (46.8)	−5.91 ± 0.01 (45.5)
Na^+	−3.12 ± 0.07 (53.9)	−3.20 ± 0.06 (56.5)	−3.63 ± 0.23 (56.3)	−2.60 ± 0.05 (45.6)	−2.74 ± 0.09 (43.7)	−5.94 ± 0.00 (46.1)
Ca^{2+}	−5.68 ± 0.04 (24.2)	−5.86 ± 0.04 (26.8)	−6.24 ± 0.24 (27.2)	−3.58 ± 0.03 (28.6)	−3.78 ± 0.06 (29.7)	−6.88 ± 0.00 (29.0)
Et_4N^+	1.50 ± 0.04 (60.0)	2.28 ± 0.04 (60.1)[a]	2.02 ± 0.31 (60.7)[a]	4.10 ± 0.03 (68.7)[a]	3.45 ± 0.07 (65.0)[a]	0.90 ± 0.04 (62.5)[a]

[a] Concentration range: 10^{-3}–10^{-4}M Et_4N^+.

Table 3

Potentiometric selectivity coefficients, log K^{pot}_{AgJ}, and response slopes (in parentheses; concentration ranges: 10^{-3}–10^{-5}M for Ag^+ and Et_4N^+, 10^{-2} to 10^{-4}M for all other ions) obtained with the separate solution method for PVC membranes based on the ionophores **VII**–**X** (cf. Fig. 2)

Ion J	VII	VIII	IX (*o*-NPOE)	IX (DOS)	X (*o*-NPOE)	X (DOS)
Ag^+	0 (59.1)	0 (57.6)	0 (61.2)	0 (61.6)	0 (60.5)	0 (61.5)
H^+	−8.92 ± 0.14 (48.1)	−10.88 ± 1.52 (52.1)	−10.17 ± 0.12 (47.0)	−7.37 ± 0.01 (57.7)	−6.74 ± 0.01 (54.5)	−6.61 ± 0.04 (58.2)
Na^+	−9.04 ± 0.13 (46.3)	−11.46 ± 0.65 (57.7)	−10.32 ± 0.13 (41.5)	−7.90 ± 0.02 (59.0)	< −9.62 (−0.2)	−8.00 ± 0.02 (46.2)
K^+	−7.12 ± 0.10 (54.3)	−7.69 ± 0.12 (53.4)	−8.44 ± 0.21 (56.9)	−7.50 ± 0.02 (57.9)	−8.16 ± 0.05 (33.5)	−7.51 ± 0.02 (52.3)
Mg^{2+}	−10.12 ± 0.17 (24.1)	−10.89 ± 0.15 (27.7)	−11.44 ± 0.23 (27.5)	−11.01 ± 0.04 (12.2)	< −10.54 (−9.9)	< −10.74 (2.3)
Ca^{2+}	−10.17 ± 0.14 (28.2)	−12.78 ± 0.12 (27.8)	−11.29 ± 0.12 (27.6)	−10.71 ± 0.04 (18.2)	< −10.46 (3.6)	< −10.43 (7.9)
Cu^{2+}	−9.01 ± 0.21 (24.4)	−8.19 ± 0.24 (16.6)	−11.08 ± 0.22 (20.5)	−10.13 ± 0.04 (30.0)5	−9.14 ± 0.04 (21.8)	−9.19 ± 0.02 (30.4)
Hg^{2+}	−2.67 ± 0.15 (60.9)[b]	not measured[a]	−3.54 ± 0.12 (35.6)	−2.58 ± 0.04 (35.0)	−4.68 ± 0.02 (43.5)[b]	−3.90 ± 0.02 (34.7)
Pb^{2+}	−8.68 ± 0.19 (32.3)	−9.20 ± 0.13 (33.2)	−10.41 ± 0.22 (35.0)	–	−8.56 ± 0.03 (46.5)	–
Et_4N^+	−3.04 ± 0.08 (68.4)	−4.77 ± 0.13 (60.6)[a]	−3.47 ± 0.02 (65.4)	−4.35 ± 0.01 (61.3)	−3.65 ± 0.02 (63.3)	−4.63 ± 0.01 (59.4)

[a] Strongly drifting signals.

[b] For the concentration range of 10^{-2}–10^{-3}M.

Table 4

Formal complex formation constants, log β, of Ag^+ obtained for ionophores **I**–**X** in PVC membranes assuming a 1:1 stoichiometry of their complexes with Ag^+ (S.D. for $n = 3$ unless indicated otherwise)

Ionophore	From selectivity data (*o*-NPOE)	Sandwich membrane technique (*o*-NPOE)	Ionophore	From selectivity data (*o*-NPOE)	Sandwich membrane technique (*o*-NPOE)	From optode responses (DOS)
I	5.86 ± 0.04	6.93 ± 0.05[a]	**VI**	6.41 ± 0.04		
II	5.07 ± 0.04		**VII**	10.39 ± 0.08	9.93 ± 0.04	
III	5.50 ± 0.03		**VIII**	12.14 ± 0.13	11.02 ± 0.07[b] 9.22± 0.04[c]	8.9 [31]
IV	3.30 ± 0.07		**IX**	10.85 ± 0.14	11.31 ± 0.10[a]	7.8
V	3.89 ± 0.07		**X**	11.00 ± 0.03	11.32 ± 0.17[a]	9.7

[a] $n = 4$.

[b] $n = 2$.

[c] DOS/PVC [31].

Table 5

Selectivity coefficients, log $K^{\mathrm{Osel}}_{\mathrm{AgJ}}$, and exchange constants, log $K^{\mathrm{Ag}}_{\mathrm{exch}}$, for Ag^+-selective fluorescent bulk optode microspheres

Ion	IX		X	
	log $k^{\mathrm{Osel}}_{\mathrm{AgJ}}$; pH 7.4, α = 0.5	**log $K^{\mathrm{Ag}}_{\mathrm{exch}}$**	**log $k^{\mathrm{Osel}}_{\mathrm{AgJ}}$; pH 7.4, α = 0.5**	**log $K^{\mathrm{Ag}}_{\mathrm{exch}}$**
Ag^+	0[a]	−1.0	0[b]	0.9
Li^+	−7.1	−8.1	−10.0	−9.1
Na^+	−8.0	−9.0	−9.2	−8.3
K^+	−7.8	−8.8	−9.1	−8.2
Mg^{2+}	−9.6	−18.3	−12.6	−19.4
Ca^{2+}	−8.1	−16.8	−9.9	−16.7
Cu^{2+}	−6.6	−15.3	−7.3	−14.2
Cd^{2+}	−8.3	−17.0	−8.2	−15.0
Hg^{2+}	−3.5	−12.3	−3.8	−10.7

[a] Lower detection limit: 5×10^{-9} M Ag^+.

[b] Lower detection limit: 2×10^{-11} M Ag^+.